CHARACTERISATION OF DRIVING RAIN EXPOSURE IN INDIA USING DAILY GRIDDED DATA

Pankaj Narula[1], Kaustav Sarkar[2]

1. School of Mathematics, TEIT Patiala, India
2. School of Engineering, IIT Mandi, India

ABSTRACT. Estimation of driving rain exposure at finer spatial resolutions facilitates a reliable consideration of potential moisture loads in the design of efficient building envelopes. Despite of its known significance, a very little has been done towards the rain exposure zones in India and elsewhere. Until recently, the only available work for Indian subcontinent was limited to the classification of 350 discrete locations based on monthly climatic records. Lately, the necessity of having a spatially continuous driving rain exposure map for India has led to the development of driving rain index (*aDRI*) maps based on daily and monthly gridded wind and rainfall data ($1^0 \times 1^0$ - lat./long. resolution). These maps are indicative of the average driving rain loads at a gridded scale. The present work enriches the existing classification through the mapping of the absolute airfield spell index (AASI) using 60-years (1951–2010) of $1^0 \times 1^0$ gridded data. AASI represents of the worst loading likely to occur in a 3-year period based on Gumbel distribution. The conjunction of these two indices would facilitate a better characterization of driving rain exposure in India. The discourse concludes with a statistical analysis of yearly indices to deduce the magnitude and significance of the trends pertinent to individual grids.

Keywords: Driving rain index, Absolute airfield spell index, Gridded data, India

Dr Pankaj Narula is a Lecturer in the School of Mathematics at TIET. His research interests are climate data analysis and mathematical modeling of infectious diseases.

Dr Kaustav Sarkar is an Assistant Professor in the School of Engineering at IIT Mandi. His area of interest includes computational modeling of transport process in concrete, soft computing, optimum design and sustainable concrete production.

INTRODUCTION

Construction materials used in building facades are often porous in nature and thus imbibe moisture from the ambient environment. The wetting of building facades leads to the gradual degradation of its performance and increase in the maintenance costs. The common forms of physical damage includes cracking and spalling of surface-layers, loss of structural integrity due to the contraction and expansion induced by wetting-drying cycles and increased vulnerability to the corrosion [1-4]. Furthermore, reduction of energy efficiency, promotion of microbial growth and poor indoor air quality are among the other significant impacts of moisture accumulation in the building materials [5-7]. The pertinence becomes more crucial for the intense moisture loading conditions of tropical regions [8].

The co-occurrence of wind gusts and rain generates an oblique vector of driving rain which is one of the primary reasons of wetting and water penetration in building facades. The need to design robust building envelope has led researchers towards the devolvement of numerical, empirical and semi-empirical techniques for the characterization of driving rain [9]. Studies based on numerical analysis and field based records have demonstrated asymmetric character of driving rain distribution over windward facades wherein the top corners were reported to be most vulnerable followed by the top and side edges [10]. CFD simulations incorporating various factors such as rain-drop size distribution and wind flow were performed to constitute catch ratios illustrating the distribution of impinging flux on various parts of the façade. Some studies have also analyzed other significant aspects such as raindrop physics, absorption, evaporation, bouncing and spreading of raindrops on exposed surface, runoff generation and moisture penetration [11-14]. These findings may provide further insights into the heat-air-moisture (HAM) simulations in the future.

Field based studies of driving rain have observed a proportional relationship of wind driven rain intensity to the wind speed and horizontal rainfall intensity [15-16]. The annual driving rain index *aDRI,* has thus been defined as the product of average wind speed and average total rainfall, as a measure of the severity of wind-driven rain intensity. This proposition has led to the constitution of driving rain maps for several countries over the globe [17-27]. These maps depict the spatial distribution of *aDRI* values across different locations with its accuracy depending upon the temporal resolution of the wind and rainfall data. For India, a country with diverse climate zones including cold, hot and dry, warm and humid, temperate and composite regions, a driving rain map is of great significance.

The *aDRI* values used to form driving rain maps can be computed using data of different temporal resolutions such as minute, hourly, daily or monthly depending upon their availability. *aDRI* values determined with finer temporal resolution dataset, owing to their capability to capture information of co-occurring wind and rainfall events at a greater detail, facilitate better estimates of driving rain conditions [28]. However, inadequate availability of climate datasets of finer resolution at several locations constrain the use of daily, monthly or annual data to determine the *aDRI*, represented respectively as *daDRI, maDRI* and *aaDRI* with increasing magnitude of errors [22, 24]. Semi-empirical models (Cosine projection approach) have also been widely used to measure the exact moisture loads inflicted on the facades with different orientation. However, it requires the wind direction in conjunction with wind speed and rainfall data. Such directional indices can be computed over different periods from individual wet spells to a year. The accuracy of directional indices also bears a positive relationship with the temporal resolution of the climate data under consideration. The limited availability of wind direction data further impels to modify the directional index into a scalar

index [22]. Alluding to the short time periods, this scalar index (I_{as}) gives an estimate that supplements the annual disposition of driving rain index. In other words, *aDRI* values represent average annual driving rain load, whereas I_{as} is indicative of the instantaneous load incident on the facades [22].

The present paper utilizes gridded data to develop the driving rain map of India. The gridded map provides complete spatial coverage and is particularly helpful to designers concerned with locations for where station based records are not available. A scalar index of driving rain, representing the short term risk of water penetration, has also been computed at gridded scale. The study utilizes data pertaining to a sixty-year period (1951–2010). The records of rainfall were obtained from the archives of India Meteorological Department (IMD) while those for wind were obtained from the web-repository of National Oceanic & Atmospheric Administration (NOAA) Earth System Research Laboratory, USA.

DATA

Climatic variables such as rainfall and wind speed are measured at meteorological stations. The data recorded at these stations are interpolated using various techniques and transformed to evenly spaced grid-points that prevails over the grids. The interpolated values at these points are indicative of average climatic conditions that prevail over the respective grids. The gridded data for the regions with meager station-based records is generated using non conventional sources such as satellites and observations from ships. Furthermore, records from several sources enable to tackle the problem of missing values and identification of outliers.

The daily gridded datasets of rainfall and wind, at $1^0 \times 1^0$ spatial resolution over the period 1951-2010, have been used in this study. The data set contains 357 grids, covering the entire geographical stretch of the Indian subcontinent. For each grid a total of 21915 daily records of wind and rainfall are used to compute the indices. The gridded data set of rainfall was procured from IMD, whereas the wind dataset, originally available at $2.5^0 \times 2.5^0$ resolution, was retrieved from the web repository of NOAA [29-32]. In order to match the resolution of rainfall dataset, the wind data was re-gridded to $1^0 \times 1^0$ using bilinear interpolation [33]. The re-gridding has been performed in openly available statistical software R [34]. A detailed discussion of generation process, interpolation technique, conventional and non conventional sources of gridded datasets is available with Narula et al [26].

METHODOLOGY

Calculation of *daDRI*

The analysis utilizes daily gridded data to determine *daDRI*. The scheme of calculation has been adopted from earlier works reported in literature. The *daDRI* for a grid can be calculated as

$$daDRI = (1/N)\sum_{i=1}^{l} W_{d_i} R_{d_i} \qquad (1)$$

Here, *daDRI* is in m^2/s, *N* is number of years and '*l*' is number of days in *N* years. W_{d_i} (*m/s*) and R_{d_i} (*m*) represent the average wind speed and total rainfall respectively on the *i-th* day

Scalar estimation of the airfield spell index from daily gridded data over India

The inclusion of direction in the computation of wind driven rain index provides more precise estimation of driving rain conditions. Airfield index (I_s) is one such index, proposed by the standard ISO 15927-3:2009, which indicates driving rain exposure particularly over the time intervals shorter than a year [22]. The index I_s (*mm/spell*) determines the maximum expected value of driving rain through the envelope during the intense rainfall spell. For a particular orientation, each such spell begins with a rainy hour and ends with a specific rainy hour subsequent to which no driving rain is observed for at least 96 hours. In other words, a rainy spell is defined as a spell which starts from rainy hour and prevails until it is interrupted by a period of 96 or more consecutive hours of no rain. Therefore, rainy spells observed over a year are separated by the 96 or more consecutive hours of rain. To this end, the driving rain during each spell of a year $I_{y,s}$ is estimated using hourly rainfall (R_h), wind speed (W_h) and wind direction (θ) corresponding to the given orientation (α) using eq. 2.

$$I_{y,s} = (2/9)\sum W_h (R_h)^{8/9} \cos(\theta - \alpha) \qquad (2)$$

After determining the maximum value of $I_{y,\,s}$ for each year ($I_{max,\,y,\,s}$), a reference value from $I_{max,\,y,\,s}$ is obtained as maximum expected value of driving rain for 3-year return period and is denoted by $I_{s.}$

Due to unavailability of adequate hourly data and wind directions, a modified version of spell index, namely the absolute spell index, is calculated over periods delimited by four or more consecutive days of no driving rain. The cosine of directional component present in the eq. (2) is replaced by its maximum value which is equal to one. This moderation provides slightly overestimated values of the spell index. The equation for absolute spell index can be represented as:

$$I_{y,\,as} = (2/9)\sum W_d (R_d)^{8/9} \qquad (3)$$

Here, W_d (*m/s*) and R_d (*mm*) represent the daily mean wind speed and the daily mean rainfall respectively. Using eq. (3) the driving rain is calculated for each absolute spell over a year ($I_{y,\,as}$) and the maximum value is identified ($I_{max,\,y,\,as}$). At each grid, a historical series of 60 maximum values of absolute spell is thus generated. Finally, maximum value of driving rain, expected over a return period of 3-year, is estimated on the basis of Gumbel distribution and denoted as I_{as}. The estimation process of maximum expected value of driving rain has been demonstrated in the subsequent section.

RESULTS

Lacy's framework has been adopted to develop the driving rain map of India. Based on *daDRI* (m^2/s) values, the exposure classes have been categorized as "shielded" for the range of [0, 3), as "moderate" for [3, 7), as **"**high" for [7, 11) and "severe" for values greater than 11 as proposed by the Lacy [35]. A station based driving rain map of India, developed by

Chand and Bhargava, is available in the literature [19]. However, quite recently, wind driven rain maps of India have been developed by Narula et al. using gridded data [26]. The maps developed in this endeavor are an advancement over the previous work in terms of temporal resolution and spatial coverage of the data. In a subsequent work, the authors further refined the estimates of driving rain index using the daily gridded data [27]. The present work is extended to the estimation of absolute spell index along which complements the average annual driving rain index reported previously. The *daDRI* map of India has been computed at $1^0 \times 1^0$ gridded scale using eq. (1) has been illustrated in Figure 1 [27].

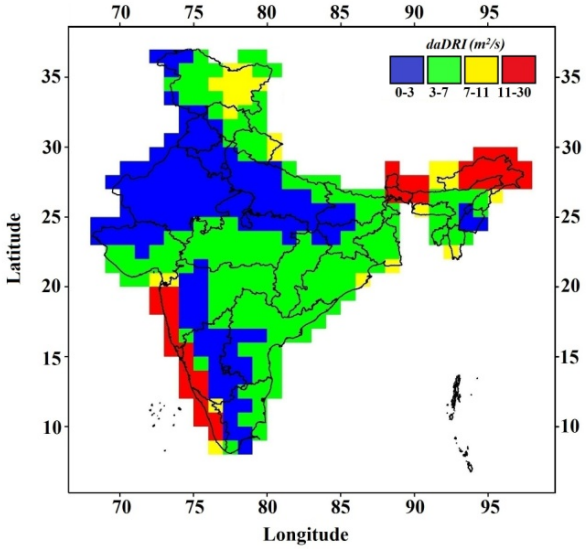

Figure 1 Driving rain map of India using *daDRI* values

The *daDRI* values, pertaining to the shielded range, are largely lie in the north-western (Punjab and Rajasthan), northern (Haryana and Uttar Pradesh) and some parts in peninsular regions (Maharashtra, Karnataka and Tamil Nadu) of India. The remaining regions (Himachal, Uttarakhand, Bihar, Jharkhand, Orissa, Madhya Pradesh, Chhattisgarh, Tamil Nadu, Andhra Pradesh, West Bengal and lower north eastern region) bear a moderate exposure except the western and a few grids on the eastern coastal region. Few grids over higher northern latitudes (Jammu and Kashmir) and north-eastern region (Sikkim and Arunachal Pradesh) experience severe to high exposure levels. Based on the distribution of *daDRI* values over the grids, 36.41%, 46.50%, 6.72% and 10.37% of the total land area can be seen pertaining to the shielded, moderate, high and severe categories of driving rain exposure respectively.

The values of maximum driving rain expected during 3-year return period have been computed using the procedure described in the previous section. The computation process is being illustrated for a typical grid with the calculated values of yearly maximum driving rain during a spell ($I_{max,\ y,\ as}$) furnished in Table 1 and the estimated parameters of Gumbel distribution shown in Table 2.

Table 1 $I_{max,\,y,\,as}$ *mm/spell* values at the grid point 77.5 ^{0}E-8.5^{0}N over the period 1951-2010

YEAR	$I_{max,\,y,\,as}$	YEAR	$I_{max,\,y,\,as}$	YEAR	$I_{max,\,y,\,as}$	YEAR	$I_{max,\,y,\,as}$	YEAR	$I_{max,\,y,\,as}$
1951	313.89	1963	230.30	1975	660.74	1987	231.11	1999	412.99
1952	291.70	1964	493.58	1976	336.96	1988	221.49	2000	354.09
1953	244.84	1965	194.95	1977	402.55	1989	298.83	2001	473.75
1954	243.11	1966	398.58	1978	551.01	1990	356.71	2002	196.60
1955	215.89	1967	312.60	1979	369.96	1991	540.16	2003	208.83
1956	111.77	1968	585.66	1980	302.24	1992	275.57	2004	279.18
1957	617.35	1969	278.01	1981	373.80	1993	349.30	2005	1520.03
1958	440.56	1970	501.46	1982	321.95	1994	261.50	2006	211.26
1959	596.77	1971	548.76	1983	102.45	1995	291.29	2007	224.68
1960	431.60	1972	490.48	1984	286.36	1996	233.14	2008	160.94
1961	1459.4	1973	755.51	1985	428.80	1997	191.67	2009	182.51
1962	389.03	1974	794.43	1986	235.90	1998	344.53	2010	142.62

Table 2 Parameters computed from the $I_{max,\,y,\,as}$ values at the grid point 77.5 ^{0}E-8.5^{0}N

PARAMETERS	VALUE
N (Number of years)	60
$\bar{X}$ (Average of maximum values of N years)	387.93
σ_X (Standard deviation of maximum values of N years)	254.77
$\bar{Y}$ (Data average of 1 to N y_i values, where $y_i = -ln(ln(N+1/i))$)	0.55
σ_Y (Standard deviation of y_i values, where $y_i = -ln(ln(N+1/i))$)	1.17
Mo (Mode = $\bar{X} - \bar{Y}(\sigma_X/\sigma_Y)$)	268.19
α (Dispersion parameter = (σ_Y/σ_X))	0.004
$F(X;Mo,\alpha) = e^{-e^{\alpha(x-Mo)}}$ (Cumulative density function)	
r (Return period)	3 years
$1-F(X;Mo,\alpha)$ (Probability of exceeding the x value)	0.33
I_{as} (likely to occur once every 3 years in *mm/absolute spell*)	**463.98**

The above procedure has been replicated to all the grids and I_{as} values have been obtained for each grid. These values have been segregated in four classes on the basis of quartiles and illustrated in Figure 2. The values of I_{as}*(mm/spell)* ranges from 38 to 3852. At first glance, it seems that each category of I_{as} should bear a match to its respective category of driving rain index. However, it is evident from Fig. 2 that regions of each category of driving rain index contain similar and more severe values of $I_{as.}$ For example, the shielded regions of driving rain index situated in northern and southern parts of India contain the regions pertaining to the shielded and moderate values of I_{as}. Similar patterns are more conspicuous for the regions with moderate and high *daDRI* values where proportion of high and severe values of I_{as} is much greater. The obtained pattern of I_{as} exhibits the footprints of climate change over the subcontinent. Several researchers have reported the impact of climate change on the Indian rainfall in terms increased frequency of short and intense rainfall events. Similar patterns can

be seen in the present analysis where maximum expected values of driving rain with 3-year return period over spell is equal or more severe than their corresponding *daDRI* values except at few grids located over higher latitudes of northern India. The identification of regions with lower *daDRI* and higher I_{as} values provide additional information to the designer.

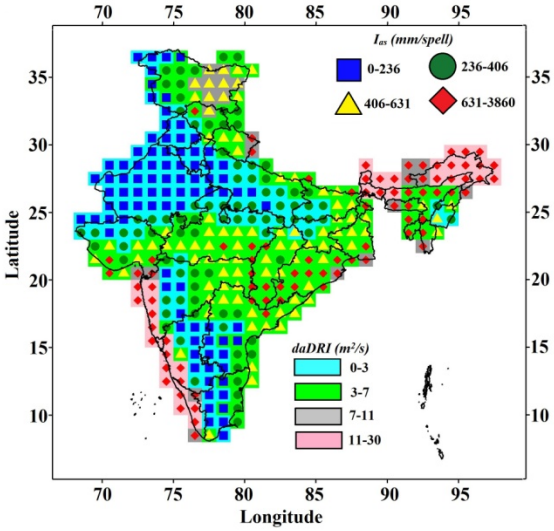

Figure 2 Spatial distribution of absolute spell index (I_{as}) over India

Trend of yearly driving rain index

The yearly driving rain index (*dyDRI*) for a particular year is calculated as:

$$dyDRI = \sum_{i=1}^{k} W_{d_i} R_{d_i} \qquad (4)$$

where, *k* represents the number of days of driving rain in the year under consideration. *dyDRI* (m^2/s) was determined for of the sixty years and for all the 357 grids. The trends were quantified based on Sen's slope estimator and Mann-Kendall's $|Z|$. The values of Sen's slope were found to be in the range [-0.20, 0.03] [36-37].

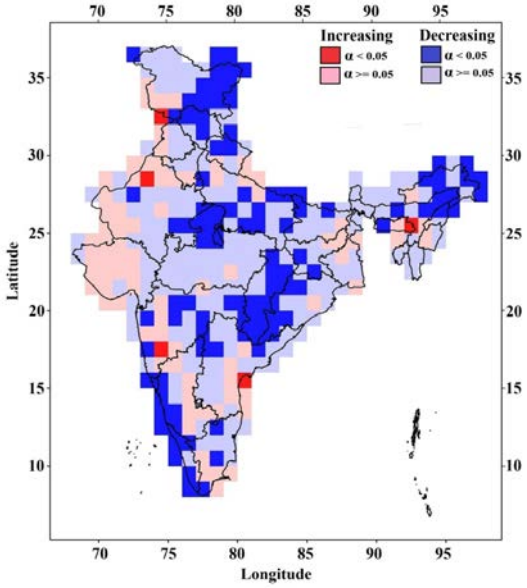

Figure 3 Trends in *dyDRI* at 95% confidence level

Figure 3 depicts the positive and negative values of Sen's slope of *dyDRI* at each grid along with their significance level at α = 0.05 (i.e. 5%). It can be inferred from the Figure 3 that, *dyDRI* bears decreasing trend across a large portion of India including the regions of Jammu Kashmir, Arunachal Pradesh, Assam, Sikkim, Nagaland, Delhi, Punjab, Himachal Pradesh, Uttar Pradesh, Madhya Pradesh, east-coast of Maharashtra, Kerala, and Karnataka. Significant increasing trend in *dyDRI* is observed over very few grids. These results conform to the previous findings of decreasing rainfall trends due to the impact of climate change across the subcontinent [38-40]. These observations indicate the declining moisture loading on exposed building facades, but, do not represent the reduction in overall severity which also includes the impact of other factors such as relative humidity and temperature.

Trend of absolute yearly maximum driving rain over spells ($I_{max,\,y,\,as}$)

The trend of absolute yearly maximum driving rain over spells ($I_{max,\,y,\,as}$) has been estimated at gridded scale and shown in the Figure 4. The positive and negative values of Sen's slope has been classified along with significance level at α = 0.05 (i.e. 5%). The range of Sen's slope values vary from -22 to 5 which indicate a much steeper decline in the values of $I_{max,\,y,\,as}$ over the period of 1951-2010. The increasing trend of $I_{max,\,y,\,as}$ can be largely observed over the Peninsular, northwestern and some parts of northeastern of the subcontinent.

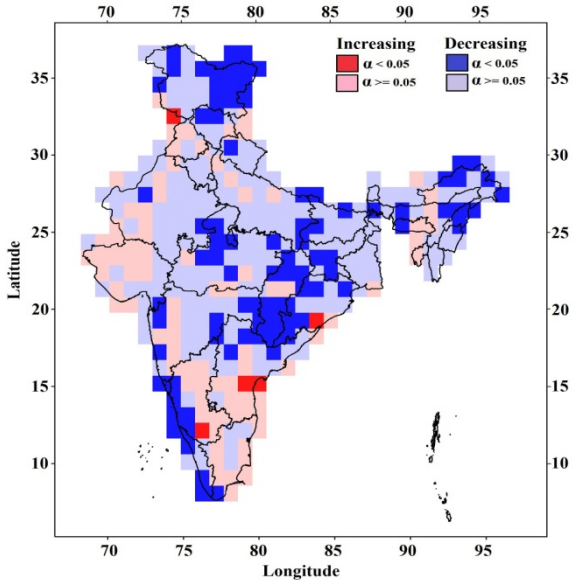

Figure 4 Trends in $I_{max,\,y,\,as}$ at 95% confidence level

CONCLUDING REMARKS

Moisture accumulation in building facades leads to their gradual deterioration and consequently in the escalation of maintenance costs. The estimation of driving rain index is important in this regard owing to its direct relevance to the improvement of the facet of design. A driving rain map based on station data depicts the exposure levels at discrete locations. The map illustrated in the present work addresses the limitation of a conventional map by the virtue of its spatial continuity. The absolute spell index provides information of worst driving rain conditions and thus complements the conventional driving rain index. The major findings and contributions of the study are summarized as under:

- The *daDRI* values presented in this work provide better estimates of average driving rain conditions in India owing to finer temporal resolution and longer temporal coverage. The gridded map also offers the advantage of spatial continuity.
- I_{as} are estimates of worst driving rain flux for a three year return period. Hence, these values provide valuable information to aid efficient design of building facades to withstand short term but intense exposure.
- *daDRI* and I_{as} maps can be used in conjunction to estimate the magnitude of driving rain severity for any location in India.
- The trends of *dyDRI* and $I_{max,\ y,\ as}$ have been observed to be decreasing over several regions of India. This conforms to the widely reported phenomena of receding monsoonal rains owing to climate change.
- A limitation of the study lies in the re-gridding of coarser wind data which may have produced some error due to interpolation. The observation, however, does not connote to the reduction of overall exposure severity which also depends on drying conditions.

REFERENCES

1. IDORN G M, Expansive mechanisms in concrete, Cement Concrete Research, 1992, Vol 22, No 6, pp 1039–1046.
2. CHAROLA A E, Salts in the deterioration of porous materials: an overview, Journal of American Institute for Conservation, 2000, Vol 39, No 3, pp 327–343.
3. ANDRADE C, ALONSO C, AND SARRIA J, Corrosion rate evolution in concrete structures exposed to the atmosphere, Cement Concrete Composites, 2002, Vol 24, No 1, pp 55–64.
4. BENAVENTE D, CULTRONE G, AND GOMEZ-HERAS M, The combined influence of mineralogical, hygric and thermal properties on the durability of porous building stones, European Journal of Mineralogy, 2008, Vol 20, No 4, pp 673–685.
5. BORNEHAG C G, BLOMQUIST G, GYNTELBERG F, JARVHOLM B, MALMBERG P, NORDVALL L, AND SUNDELL J, Dampness in buildings and health, 2001, Indoor Air, Vol 11, No 2, pp 72–86.
6. GAYLARDE C, SILVA M R, AND WARSCHEID T H, Microbial impact on building materials: an overview, Materials and Structures, 2003, Vol 36, No 5, pp 342–352.
7. BHATTACHARJEE B, Moisture influence on the thermal properties of materials in building envelopes and sustainability in tropical climates. In: ICSDEC 2012 Developing the Frontier of Sustainable Design, Engineering, and Construction, 2013, pp 765-774.
8. ABUKU M, JANSSEN H, AND ROELS S, Impact of wind-driven rain on historic brick wall buildings in a moderately cold and humid climate: numerical analyses of mould growth risk, indoor climate and energy consumption, Energy and Buildings, 2009, Vol 41, No 1, pp 101–110.
9. BLOCKEN B, AND CARMELIET J, A review of wind-driven rain research in building science, Journal of Wind Engineering and Industrial Aerodynamics, 2004, 92 (13), pp 1079–1130.
10. KARAGIOZIS A, HADJISOPHOCLEOUS G, AND CAO S, Wind-driven rain distributions on two buildings, Journal of Wind Engineering and Industrial Aerodynamics, 1997, Vol 67-68, pp 559–572.

11. ABUKU M, BLOCKEN B, AND ROLES S, Moisture response building facades to wind driven rain: field measurements compared with numerical simulations, Journal f Wind Engineering and Industrial Aerodynamics, 2009A, Vol 97, No 5–6, pp 197–207.
12. ABUKU M, BLOCKEN B, POESEN J, AND ROELS S, Spreading, splashing and bouncing of wind-driven raindrops on building facades, 11th Americas Conference on Wind Engineering. San Juan, Puerto Rico. June 2009B, pp 22-26.
13. ABUKU M, JANSSEN H, POESEN J, AND ROELS S, Impact, absorption and evaporation of raindrops on building facades, Building and Environment, 2009C, Vol 44, No 1, pp 113–124.
14. BLOCKEN B, DEROME D, AND CARMELIET J, Rainwater runoff from building facades: a review, Building and Environment, 2013, Vol 60, pp 339–361.
15. HOPPESTAD S, Slagregn I Norge (Driving Rain in Norway, in Norwegian), 1955, Vol. 13, NBI Report
16. LACY R E, Driving-rain Maps and the Onslaught of Rain on Buildings, 1965, Building Research Station.
17. LACY R E, Driving Rain at Garston, United Kingdom, 1964, Building Research Station.
18. SAUER P, An annual driven rain index for China, Building and Environment, 1987, Vol 22, No 4, pp 239–240.
19. CHAND I, AND BHARGAVA P K, Estimation of driving rain index for India, Building and Environment, 2002, Vol 37, No 5, pp 549–554.
20. SAHAL N, Proposed approach for defining climate regions for Turkey based on annual driving rain index and heating degree-days for building envelope design, Build. Environ, 2006, Vol 41, No 4, pp 520–526.
21. GIARMA C, AND ARAVANTINOS D, Estimation of building components' exposure to moisture in Greece based on wind, rainfall and other climatic data, Journal of Wind Engineering and Industrial Aerodynamics, 2011, Vol 99, No 2, pp 91–102.
22. PEREZ-BELLA J M, DOMÍNGUEZ-HERN ANDEZ J, RODRÍGUEZ-SORIA B, DEL COZ-DÍAZ J J, AND CANOSUNEN E, Estimation of the exposure of buildings to driving rain in Spain from daily wind and rain data, Building and Environment, 2012, Vol 57, pp 259–270.
23. PEREZ-BELLA J M, DOMÍNGUEZ-HERN ANDEZ, J., CANO-SUN~EN, E., DEL COZ-DÍAZ, J.J., ALONSOMARTÍNEZ, M., Global analysis of building façade exposure to water penetration in Chile, Building and Environment, 2013, Vol 70, pp 284–297.
24. GIARMA C, AND ARAVANTINOS D, On building components' exposure to driving rain in Greece, Journal of Wind Engineering and Industrial Aerodynamics, 2014, Vol 125, pp 133–145.
25. PEREZ-BELLA J M, DOMÍNGUEZ-HERN ANDEZ J, CANO-SUNEN E, DEL COZ-DÍAZ J J, AND MARTÍNRODRÍGUEZ A, Procedure for a detailed territorial assessment of wind-driven rain and driving-rain wind pressure and its implementation to three Spanish regions, Journal of Wind Engineering and Industrial Aerodynamics, 2014, Vol 128, pp 76–89.
26. NARULA P, SARKAR K, AND AZAD S, Driving rain indices for India at $1^0 \times 1^0$ gridded scale, Journal of Wind Engineering and Industrial Aerodynamics, 2017, Vol 161, pp 1–8.

27. NARULA P, SARKAR K, AND AZAD S, Indexing of driving rain exposure in India based on daily gridded data, Journal of Wind Engineering and Industrial Aerodynamics, 2018, Vol 175, pp 244–251.
28. BLOCKEN B, AND CARMELIET J, On the errors associated with the use of hourly data in wind-driven rain calculations on building facades, Atmospheric Environment, 2007, Vol 41, No 11, pp 2335–2343.
29. KALNAY ET AL., The NCEP/NCAR 40-year reanalysis project, Bulletin of American Meteorological Society, 1996, Vol 77, pp 437–470.
30. NOAA, Earth System Research Laboratory, http://www.esrl.noaa.gov/psd/data/gridded/ data.ncep.reanalysis.derived.surface.html
31. RAJEEVAN M, BHATE J, AND KALE J D, AND LAL B, Development of a High Resolution Daily Gridded Rainfall Data for the Indian Region. IMD Meteorological Monograph No. Climatology 22/2005, 27 pp.
32. PAI D S, SRIDHAR L, RAJEEVAN M, SREEJITH O P, SATBHAI N S, AND MUKHOPADHYAY B, Development of a new high spatial resolution ($0.25^0 \times 0.25^0$) long period (1901–2010) daily gridded rainfall data set over India and its comparison with existing data sets over the region, Mausam, 2014, Vol 65, No 1, pp 1–18.
33. SHEPARD D, A two-dimensional interpolation function for irregularly spaced data, In: Proceedings of the 1968 ACM National Conference, 1968, pp 517–524.
34. R Core Team, R: a Language and Environment for Statistical Computing. R Foundation for Statistical Computing, Vienna, Austria, 2013, http://www.R-project.org/.
35. LACY R E, Climate and Building in Britain, Building Research Establishment Her Majesty's Stationery Office London, 1977, 185 pp.
36. MANN H B, Nonparametric tests against trend, Econometrica, 1945, Vol 13, pp 245–259.
37. KENDALL M G, Rank Correlation Methods, Griffin, London, 1975, UK.
38. RAMANATHAN V ET AL., Atmospheric brown clouds: impacts on South Asian climate and hydrological cycle, Proceedings of the National Academy of Sciences of the United States of America, 2005, Vol 102, pp 5326–5333.
39. TURNER A G, AND ANNAMALAI H, Climate change, and the South Asian summer monsoon, Nature Climate Change, 2012, Vol 2, No 8, pp 587–595.
40. RATHORE L S, ATTRI S D, JASWAL A K, State Level Climate Change Trends in India, IMD Meteorological Monograph No. ESSO/IMD/EMRC/02/2013.